Biomass-derived Materials for Gas Adsorption Applications

Valentina Gargiulo*, Luciana Cimino, Alessio Occhicone, Michela Alfè

CNR - STEMS Institute of Sciences and Technologies for Sustainable Energy and Mobility, P.le V. Tecchio, 80 80125 Napoli, Italy

valentina.gargiulo@stems.cnr.it

The development of technologies devoted to re-cycle and/or re-use wastes generated from the industrial processing of agricultural raw materials is a research topic attracting increasing attention. In this work, different carbonaceous biomass-derived materials were prepared with the aim of compare the performances of materials with different chemical surface properties as gas adsorbents. The final goal of the work is to highlight the advantages and disadvantages of using a real biomass as a raw material for the preparation of gas sorbents. Different biomasses were used for the preparation of gas adsorbents: chitosan and thistle (*Cirsium vulgare*) to produce N-rich char types, rice husk, lemon peels and pectin to produce O-rich char types. Chemical procedures to increase the nitrogen content as well as the surface area and the porosity of the biomass-derived materials were also applied. A selection of the obtained materials, after a deep chemico-physical characterization, has been tested for gas adsorption at high pressure in a volumetric analyzer.

1. Introduction

There are many families of advanced materials that can be grouped under the heading of porous solid sorbents: zeolites, metal–organic Frameworks (MOFs), porous organic polymers (POPs), and porous carbons. Porous carbons derived from various biomass feedstocks are widely used as CO_2 adsorbents and the research of material optimization strategies based also on suitable biomass pre-treatments has developed tremendously in the last decade. Anyway, several aspects related to the effective use of biomass-derived carbons in adsorption processes need to be addressed and explored. Adsorbents for CO_2 and CH_4 should typically exhibit high adsorption and desorption capacity, high packing density, high adsorption/desorption rate, low susceptibility to temperature changes during adsorption and desorption, hydrophobic nature, low isosteric heat of adsorption, good mechanical strength, tolerance to impurities. In addition, adsorbents should be inexpensive for the end user, be hard, not easily broken or powdered (Bernardo et al., 2021).

Biomass materials, used as precursors for producing activated carbon material, are cheap and readily available. The selection of the right synthesis and modification conditions is crucial for obtaining a sorbent with the desired properties for gas adsorption. The conversion of the biomass into porous carbons involves a carbonization (pyrolysis) process and a physical and/or chemical activation. During physical-activation the char obtained by a first thermal treatment (carbonization) in the absence of O_2 at temperatures between 400-850°C is activated with oxidant/gasifying gases like steam, air, N_2, CO_2 or their mixture at temperatures around 600-1000°C. Nevertheless, in the physical-activation there is a poorer control of the porosity development. Chemical-activation can be a one-step or two-step method since the impregnation with the activating chemical (dehydrating agents and/or oxidants) can be made directly in the biomass or in the resulting char from the first step of carbonization. After impregnation, the material (raw biomass or char) and the activating agent are heated under inert atmosphere at temperatures between 400-800°C. H_3PO_4, H_2SO_4, $ZnCl_2$, K_2CO_3, NaOH, and KOH are usually used in chemical activations of biomass precursors (Bernardo et al., 2021). Chemical-activation usually provides biomass-derived porous carbons with high surface areas and a good control of the porosity. Increasing the basicity of the carbon is the most efficient way to improve the adsorption efficiency toward CO_2 uptake (Al-Hajri et al., 2022). Adding CO_2-philic moieties, such as nitrogen containing groups within the carbon framework can improve material adsorption capacity, increase CO_2 uptake and CO_2/N_2 selectivity because of the strong interaction between the basic N-functional sites and the

acidic CO_2 molecules (Al-Hajri et al., 2022). As matter of facts, N-doped porous carbons have garnered much attention in the gas adsorption field due to the ease of preparation.

In this work different carbonaceous biomass-derived materials were produced and a selection of them tested for gas adsorption applications. With the aim of comparing the performance of materials with different chemical surface properties, chitosan, and thistle (*Cirsium vulgare*) were selected to produce N-rich char types, while rice husk, lemon peels and pectin to produce O-rich char types. Chemical procedures to increase the nitrogen content as well as both the surface area and the porosity of the biomass-derived materials were also applied. A selection of the obtained materials was then tested for CO_2, CH_4 and N_2 adsorption by using a volumetric analyser.

2. Experimental section

2.1 Materials

Citrus pectin (CP) and scrimp-derived chitosan (SC) were purchased form Merck KGaA and used without any further purification. Rice husk (RH) derived from a deposit in Kazakhstan, and it was used as received. Lemon peels (LP), recovered as waste after Limoncello liquor production process, were dried for 24 hours in a hoven at 105°C to remove alcohol traces and water and then blade milled up to a micrometric size. Thistle (TH) was kindly provided by Agriculture Department of University of Naples "Federico II" and used as received. The composition and the properties of all the used feedstocks are reported in Table 1.

Table 1: Feedstocks characteristics

	C (wt.%)	H (wt.%)	N (wt.%)	Other elements (wt.%)	Moisture (wt.%)	Volatiles (wt.%)	Ashes (wt.%)	Fixed carbon (wt.%)
TH	47.7±0.7	6.10±0.60	2.78±0.30	34.4±1.0	0.46±0.01	74.7±0.2	4.84±0.20	20.0±0.03
CP	40.2±0.9	4.10±0.50	-	55.7±0.5	1.87±0.30	75.8±0.5	4.53±0.70	17.8±0.6
LP	39.2±0.8	5.20±0.10	1.10±0.20	54.5±1.0	1.75±0.10	76.2±0.5	5.65±0.04	16.4±0.4
SC	38.0±0.7	6.32±0.30	5.08±0.20	50.6±1.0	1.79±0.01	71.8±0.6	0.41±0.05	26.0±0.8
RH	34.9±1.1	5.1±0.4	-	60.0±1.0	7.69±0.20	57.84±0.6	18.57±0.40	15.90±0.50

2.2 Gas adsorbent production

LP, TH, SC, CP were thermally treated in a LECO 701 thermobalance at 550°C under a nitrogen atmosphere (flux 8.5 L/min). The temperature was raised from 25°C up to 100°C applying a heating rate (HR) of 15°C/min and then held for 10 minutes to remove moisture, then the temperature was raised up to 550°C applying a HR of 37°C/min and held for 1.5 hours. At the end of the thermal treatment, the system was cooled down under nitrogen flux. RH was carbonized under an inert atmosphere (Ar) in an auger furnace in the 500–800°C temperature range for 3 hours. Carbonized rice husk (RH-char) underwent an alkaline-based desilication process (Gargiulo et al., 2019) to obtain RH-NaOH. RH-NaOH was then mixed with urea (1:1 mass ratio), ball milled (600 rpm, 10 min) and thermally treated in a LECO 701 thermobalance at 800°C under a nitrogen atmosphere (flux 8.5 L/min). The temperature was raised from 25°C up to 100 °C applying a HR of 15°C/min and then held for 10 minutes to remove moisture, then the temperature was raised up to 800°C applying a HR of 40°C/min and held for 1.5 hours. At the end of the thermal treatment, the system was cooled down under nitrogen flux. The obtained material was labelled as N-RH-NaOH.

2.3 Structural characterization methods

Proximate analysis was performed on a LECO 701 thermobalance according to the standard ASTM D7582-15. C, H, N contents of feedstocks and char samples were determined by ultimate analysis in accordance with ASTM D3176-15 standard by using a LECO 628 analyser after EDTA calibration. The thermal behaviour of the feedstocks and char samples was investigated through thermogravimetry on a Perkin-Elmer STA6000. Each feedstock (5-20 mg) was heated from 30°C up to 700°C under inert atmosphere (N_2, 40 mL/min) applying a heating rate (HR) of 5°C/min. Char samples (5-20 mg) were heated from 30°C up to 800°C under oxidizing atmosphere (air, 40 mL/min) applying a HR of 10°C/min. The surface chemistry of the char samples was investigated by infrared spectroscopy in the 450–4000 cm^{-1} range on a Perkin–Elmer Frontier MIR spectrophotometer operated in transmittance mode with KBr pellets (2 wt.%). The crystallinity of char samples was investigated by X-ray powder diffraction (XRD) analysis in the 2θ range 3–90° using a Rigaku Miniflex 600 automated diffractometer equipped with a CuKα radiation source.

2.4 Adsorption tests

The gas storage ability of a selection of materials was tested by using various probes (N_2, CO_2, CH_4) and various temperatures (from cryogenic to near ambient conditions) from vacuum up to ambient pressures, under equilibrium conditions. CO_2, CH_4 and N_2 adsorption isotherms at 0, 10 and 25 °C were collected on a volumetric analyser (Micrometrics Tristar 3020) equipped with one pressure transducer, in the pressure range of 0.1–900 Torr. During the analysis, the temperature was controlled and maintained using a water circulating bath. Before the gas adsorption experiments, all the samples were outgassed under vacuum at 120°C for 15-17 hours. Ultrapure gases were used for all the measurements. The CO_2/N_2 and CO_2/CH_4 selectivities were calculated from the single component experimental adsorption data, using the Ideal Adsorbed Solution Theory (IAST) (Myers et al., 1965). The selectivity of a gas X over Y ($S_{x/y}$) was calculated as the ratio: $S_{x/y}=(q_x/q_y)/(p_x/p_y)$ where q_x and q_y were the IAST predicted uptakes (cm^3/g) and p_x and p_y were the partial pressures of gas X and Y respectively. The CO_2 isosteric heats of adsorption were calculated using the Clausius−Clapeyron equation from the set of equilibrium isotherms acquired at near ambient conditions (0, 10, and 25°C). An average Q_{st} value was calculated over the whole range of CO_2 uptakes.

3. Results and discussion

Figure 1 shows the thermal profiles of the feedstocks up to 700°C under an inert atmosphere. LP and CP are the two feedstocks less thermally stable (their decomposition starts before 200°C), while the other feedstocks start to decompose after 250°C. Overall, the thermal decomposition can be considered concluded at 550°C for all the feedstocks leading to the production of a thermal stable solid residue (char). RH produces the high amount of solid residue (45 wt.%), while LP the lower amount (20 wt.%).
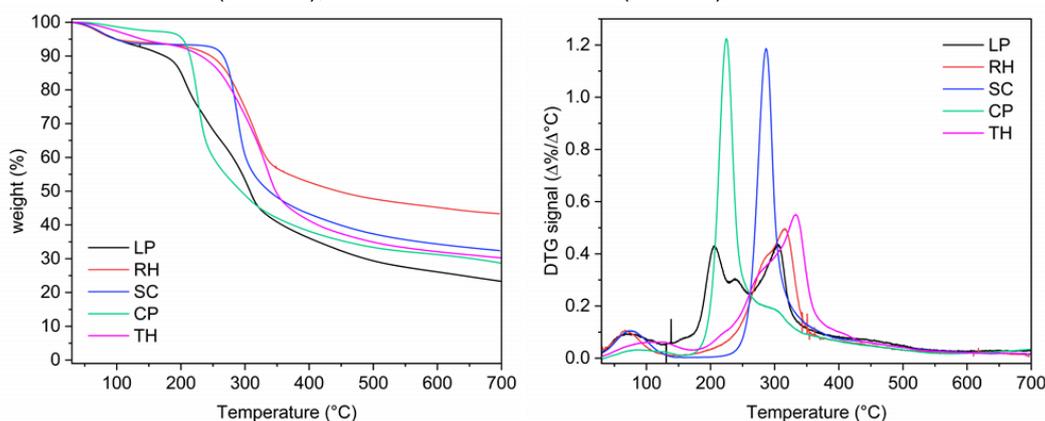
Figure 1: TG (left) and DTG (right) curves of the feedstocks (N_2,40 mL/min, HR=5°C/min)

In Table 2, the compositions in terms of C, H and N contents of all the char samples are reported while the thermal profiles under an oxidative atmosphere are shown in Figure 2. LP-char contains 55.9 wt.% of carbon and low contents of H and N (0.65 wt.% and 0.35 wt.%, respectively). LP-char is one of the less thermally stable materials among the samples examined, in fact it is completely burnt off before 500°C. This behaviour probably is the result of catalytic effects promoted by the high ash content (5.65 wt.% in the parent feedstock, Table 1). SC-char contains a fairly high carbon content (70.8 wt.%) and a very high N content (8.5 wt.%) tracing the composition of the parent feedstock (Table 1). As concerns its thermal behaviour, SC-char exhibits a thermal profile characterized by only one main event around 550°C indicating an overall structural uniformity and a quite good degree of graphitization. CP-char contains a quite high carbon content (62.8 wt.%), but very low hydrogen content (0.2 wt.%) and a negligible nitrogen content. Despite the high carbon content, CP-char is the less thermally stable material among all the investigated samples as its decomposition starts before 350°C, probably as consequence of catalytic effects exerted by the not negligible ash content (4.53 wt.% in the parent feedstock, Table 1). TH-char contains a content of carbon comparable with that of LP (56.4 wt.%) and quite high hydrogen and nitrogen contents (0.80 wt.% and 1.60 wt.%, respectively). Its thermal profile suggests a good degree of graphitization since the temperature of burn-off is around 550°C, comparable to well-structured carbonaceous materials as activated carbons and combustion derived materials (Arnal et al., 2013). RH-char is characterized by a quite low carbon content (44.5 wt.%) and a not negligible amount of hydrogen (1.10 wt.%). RH-char exhibits a quite high thermal stability, its TG profile is characterized by only

one thermal event above 550°C. RH-char as LP-char and CP-char is very rich in ash (the unburned residue accounts for the 50 wt.%).

Table 2: gas adsorbent composition

	C (wt.%)	H (wt.%)	N (wt.%)	Other elements (wt.%)
TH-char	56.4±0.3	0.80±0.6	1.60±0.3	41.2±1.1
CP-char	62.8±1.3	0.20±0.02	-	37.0±1.3
LP-char	55.9±0.4	0.65±0.20	0.35±0.30	43.1±0.8
SC-char	70.8±1.6	1.50±0.10	8.50±0.30	19.2±2.0
RH-char	44.5±1.5	1.10±0.40	-	54.4±1.3
RH-NaOH	80.3±1.3	1.10±0.20	-	18.6±1.0
N-RH-NaOH	68.6±3.0	0.05±0.08	2.25±0.10	29.1±3.0
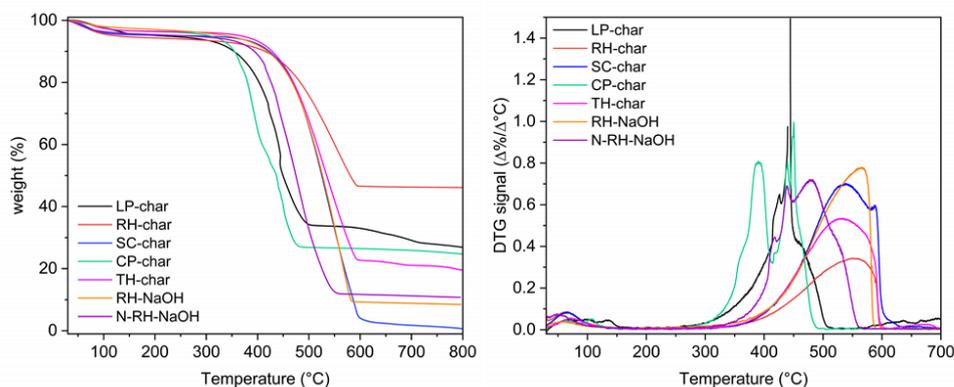
Figure 2: TG (left) and DTG (right) curves of adsorbents (air, 40 mL/min, HR=10°C/min).

The composition of the desilicated RH-char (RH-NaOH) differs from that of its precursor (RH-char) for the carbon content (80.3 wt.% vs 44.5 wt.%). The thermal behaviour of RH-NaOH is comparable to that of RH-char (the temperature of burn-off is around 550°C) but, as expected, the amount of unburned residue is quite low (below 15 wt.%). N-RH-NaOH has a lower content of carbon and hydrogen (68.6 wt.% and 0.05 wt.% respectively) and a higher content of nitrogen and other elements (2.25 wt.% and 29.1 wt.%, respectively) compared to its precursor (RH-NaOH). N-RH-NaOH is more thermally reactive than RH-NaOH (the temperature of burn-off is about 450°C) and this behaviour may be related to the milling treatment that makes the surface of the materials more reactive.

The crystallinity of the char samples was probed by XRD and the resulting patterns are reported in Figure 3 (left panel). SC-char, RH-char, RH-NaOH and N-RH-NaOH exhibit a XRD pattern typical of amorphous carbons (Arnal et al., 2013). The XRD patterns of SC-char, RH-NaOH and N-RH-NaOH contain a main broad peak around 25 2θ° while that of RH-char contains as well a main broad peak, but shifted toward lower 2θ° (the maximum is around 21 2θ°) due to the very high concentration of SiO_2 (Gargiulo et al. 2019). The XRD patterns of CP-char, TH-char and LP-char contain a broad peak around 25 2θ° ascribable to amorphous carbon and sharper peaks at higher 2θ° values ascribable to inorganic components. The main inorganic component identified in LP-char and TH-char is calcite ($CaCO_3$) while in CP-char it is natrite (Na_2CO_3).

The surface chemistry of the different char samples was investigated by infrared spectroscopy (Figure 3, right panel). RH-char FTIR spectrum contains broad peaks in the region between 1600 and 1000 cm^{-1} attributed to the skeletal vibrations of C-C, C=C and C=O bonds in complex carbon network and an intense peak at 1100 cm^{-1} ascribable to Si-O-Si stretching mode signal (Gargiulo et al. 2019). The FTIR profile changes because of the desilication process, in fact the RH-NaOH FTIR spectrum resembles that typical of an amorphous carbon with broad peaks between 1600 and 1000 cm^{-1} due to the vibration modes of the C-C, C=C and C=O bonds. The same results were obtained for N-RH-NaOH. SC-char FTIR spectrum, as well, contains broad peaks between 1600 and 1000 cm^{-1} due to the vibration modes of C-C, C=C and C=O bonds and a very small peak around 2200 cm^{-1} ascribable to N-containing groups.
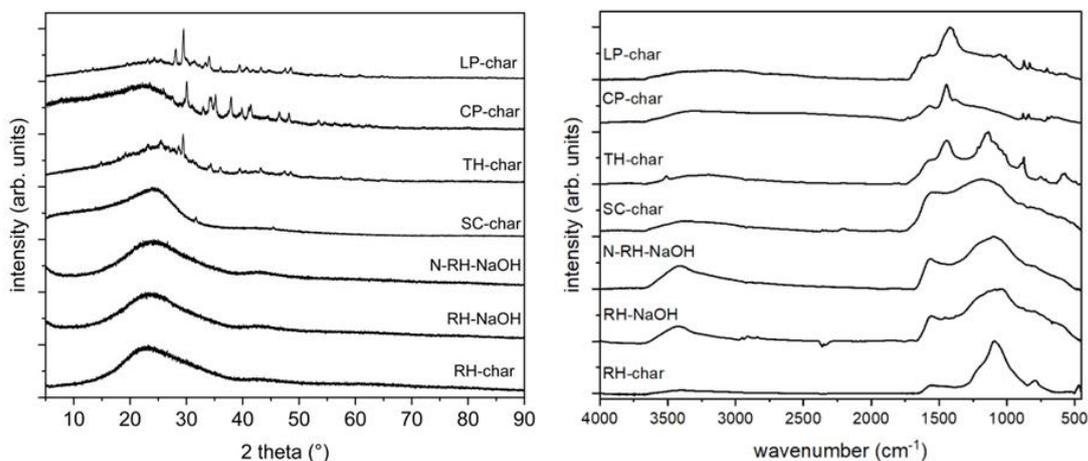
Figure 3: (left) XRD patterns of char samples. (right) FTIR spectra of char samples.

LP-char, TH-char and CP-char FTIR spectra are quite similar, all contain broad overlapping bands around 1580 cm^{-1} ascribable to the skeletal vibrations of C=C and/or C=O bonds, an intense peak around 1480 cm^{-1} and low intensity bands below 1000 cm^{-1} attributable to vibrational modes of inorganic components.

Preliminary results regarding gas adsorption capacities have been achieved probing RH-char and RH-NaOH. Gas adsorption experiments are ongoing on the other char samples described in this work. At first, the capacity to adsorb CO_2 at 0°C has been evaluated and the results are reported in Figure 4.
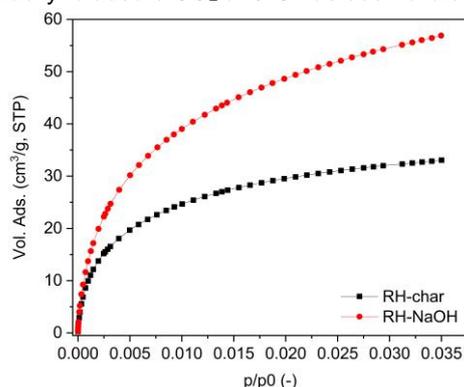
Figure 4: CO_2 isotherms of RH-char and RH-NaOH at 0°C.

For both the materials the shape of the CO_2 adsorption isotherms suggest the presence of specific interactions between CO_2 (a marked knee in the isotherm at low p/p0) testifying that both materials can act as CO_2 adsorbent. To understand better such a difference, micropore volume and size and chemical functionalization of the pores must be considered. In general, high CO_2 uptakes correspond to samples with high micropore volumes, and even if RH-char and RH-NaOH are both mesoporous materials, the desilication process allows for the removal of pore clogging and leads to an increase of microporous fraction (Gargiulo et al., 2019). Overall, the removal of ashes induces an increase of CO_2 uptake of about 31%, so between the two materials RH-NaOH was selected for further adsorption experiments. The CO_2 adsorption capacity of RH-NaOH was estimated at three different temperatures (0, 10, 25°C) and the obtained isotherms are contrasted in Figure 5 (left panel). As expected, with the increase of temperature, the adsorption capacity decreases since the adsorption process is an exothermic process. Looking at the isotherm measured at 25°C, the maximum amount of CO_2 adsorbed is between 1-2.5 mmol/g, a value comparable to literature findings on similar materials not chemically or physically activated (Gargiulo et al., 2018). The CO_2 adsorption isotherms were used to calculate the CO_2 isosteric heat of adsorption using the Clausius–Clapeyron equation. The calculated value of the isosteric heat of adsorption was ~30 KJ/mol and resulted in line with those evaluated for other biochar samples obtained by slow pyrolysis experiments (Gargiulo et al., 2018) and indicated non-specific interactions with the gas (pure physisorption process).

To better characterize the adsorption properties of RH-NaOH, CO_2, N_2 and CH_4 adsorption isotherms at 25°C were also acquired.
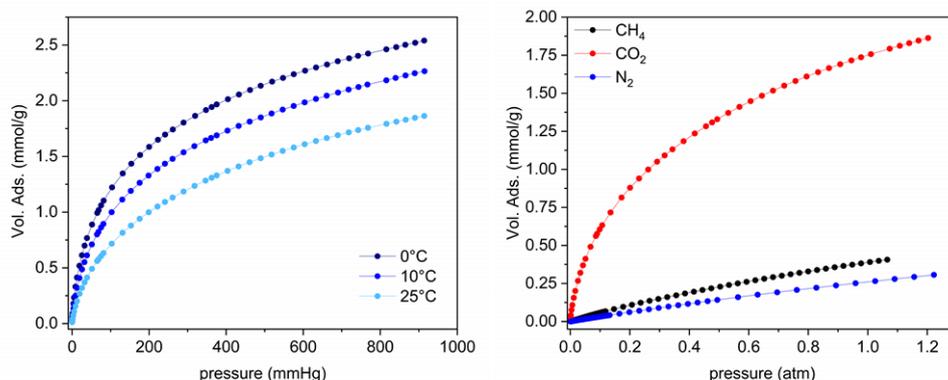
Figure 5: (left) CO_2 adsorption isotherms at 0, 10 and 25°C of RH-NaOH; (right) CO_2, N_2 and CH_4 adsorption isotherms at 25°C of RH-NaOH.

To describe better such properties, CO_2/N_2 and CO_2/CH_4 selectivities at 1 bar for binary mixtures have been evaluated. A selectivity of 31 was calculated for a CO_2:N_2 (15:85) mixture and a selectivity of 14 was estimated for a CO_2:CH_4 (30:70) mixture. Overall, these selectivity values are good and in line with those of similar materials, but lower compared to those materials rich in functionalities able to form specific interactions with CO_2 due to its acidic nature (Ren et al., 2018) . For this reason, materials containing nitrogen-based functionalities like N-RH-NaOH, TH-char and SC-char are expected to perform better in CO_2 adsorption showing higher CO_2/N_2 and CO_2/CH_4 selectivities.

4. Conclusions

In this work N-rich and O-rich char samples have been produced from agricultural/aquacultural wastes and structurally characterized. A first attempt to introduce nitrogen-containing functionalities in char was also carried out. The preliminary results obtained on the desilicated RH derived char (RH-NaOH) indicated that good adsorption performances can be achieved also in terms of selectivity toward CO_2 over N_2 and CH_4. Better CO_2 uptakes are expected to be achieved by using materials naturally containing nitrogen-based functionalities like TH-char and SC-char or those produced by chemical treatments (N-RH-NaOH).

Acknowledgments

References

Al-Hajri, W., De Luna, Y., Bensalah, N., 2022, Review on Recent Applications of Nitrogen-Doped Carbon Materials in CO_2 Capture and Energy Conversion and Storage, Energy Technology 10, 2200498.

Arnal, C., Alfe, M., Gargiulo, V., Ciajolo, A., Alzueta, M.U., Millera, A., Bilbao, R., 2013, Characterization of soot, Chapter In: F. Battin-Leclerc, J.M. Simmie, E. Blurock (Eds.), Developing Detailed Chemical Kinetic Models series: Green Energy and technology, Springer-Verlag, London, UK, 333–362.

Bernardo, M., Lapa, N., Fonseca, I., Esteves, I.A.A.C., 2021, Biomass Valorization to Produce Porous Carbons: Applications in CO_2 Capture and Biogas Upgrading to Biomethane-A Mini-Review. Frontiers in Energy Research 9, 625188.

Gargiulo, V., Gomis-Berenguer, A., Giudicianni, P., O. Ania, C., Ragucci, R., Alfè, M., 2018, Assessing the Potential of Biochars Prepared by Steam-Assisted Slow Pyrolysis for CO_2 Adsorption and Separation, Energy & Fuels, 32, 10218−10227.

Gargiulo, V., Alfè, M., Raganati, F., Zhumagaliyeva, A., Doszhanov, Y., Ammendola P., Chirone R., 2019, CO_2 Adsorption under Dynamic Conditions: An Overview on Rice Husk-Derived Sorbents and Other Materials, Combustion Science and Technology, 191(9), 1484-1498.

Myers, A. L., Prausnitz, J. M. 1965, Thermodynamics of mixed-gas adsorption, AIChE J., 11, 121−127.

Ren, X., Li, H., Chen, J., Wei, L., Modak, A., Yang, H., Yang, Q., 2017, N-doped porous carbons with exceptionally high CO_2 selectivity for CO_2 capture, Carbon, 114, 473-481.